Capillary condensation in the two-dimensional lattice gas: A Monte Carlo test of fluctuation corrections to the Kelvin equation

1997 J. Phys. A: Math. Gen. 30 3285

(http://iopscience.iop.org/0305-4470/30/10/009)

J. Phys. A: Math. Gen. **30** (1997) 3285–3297. Printed in the UK PII: S0305-4470(97)79753-1

Capillary condensation in the two-dimensional lattice gas: A Monte Carlo test of fluctuation corrections to the Kelvin equation

E V Albano†, K Binder‡ and W Paul‡

† INIFTA, Universidad de la Plata, C.C. 16 Suc. 4, (1900) La Plata, Argentina
‡ Institut für Physik, Johannes Gutenberg-Universität Mainz, Staudingerweg 7, D-55099 Mainz, Germany

Received 21 November 1996, in final form 10 February 1997

Abstract. A two-dimensional lattice gas model with nearest-neighbour attractive interaction confined in a strip of width L between two parallel boundaries at which an attractive short-range force acts is studied by Monte Carlo simulations, for cases where the system is in the wet phase near the critical wetting transition line for $L \to \infty$. We study the shift of the chemical potential μ of the transition in the strip as a function of L by thermodynamic integration methods, $\Delta\mu = \mu_c(L) - \mu_c(\infty)$, and also obtain the thickness l_c of the wetting film at the chemical potential $\mu_c(L)$ at which capillary condensation occurs. In the range $32 \leqslant L \leqslant 120$ the data are consistent with a variation according to the Kelvin equation, $\Delta\mu \propto L^{-1}$, as well as with a shifted Kelvin equation, $\Delta\mu \propto (L - L_0)^{-1}$, with a constant L_0. Thus, we find no evidence for the fluctuation correction $\{\Delta\mu \propto (L - 3l_c)^{-1}\}$ predicted by Parry and Evans. This failure is traced back to the fact that in this range of linear dimensions there are not yet any well developed wetting layers at coexistence, and the prediction $l_c \propto L^{1/3}$ from the theory of complete wetting does not hold in this range either. Instead we empirically find a relation $l_c \propto \ln L +$ constant over the whole range of system sizes we studied.

1. Introduction

In a confined geometry phase transitions get shifted (and sometimes also rounded) by finite size effects [1–7]. A particularly interesting phenomenon is the wall-induced shift of the first-order liquid–gas-type transition in thin film geometry ('capillary condensation' [7–11]), since there may occur a subtle [12–19] interplay of finite size effects and wetting phenomena (for reviews on wetting in general see [20–22]). Only in the situation where the walls (for simplicity, we discuss here only the symmetric case of confinement by two parallel and physically fully equivalent walls) are nonwet (in other words, the contact angle δ [20–22] is nonzero), the simple 'Kelvin equation' [23] is supposed to hold [7–11],

$$\Delta\mu \equiv= \mu_{\text{coex}} - \mu_c(L) = 2\sigma_{\text{lg}} \cos\delta/[L(\rho_l - \rho_g)] \qquad L \to \infty. \tag{1}$$

In equation (1), we have assumed that the condensation transition from a gas (at a bulk gas density ρ_g) to a liquid (bulk density ρ_l) occurs in a slit-like capillary of thickness L at a chemical potential $\mu_c(L)$, while in the bulk it occurs at $\mu_{\text{coex}} \equiv \mu_c(L \to \infty)$, and the interfacial tension of the (planar) liquid–gas interface is denoted as σ_{lg}.

When the walls are wet, however, for $L \to \infty$ and $\mu = \mu_{\text{coex}}$ the walls are coated by infinitely thick wetting layers (assuming an ideal case without any effects such as gravity

0305-4470/97/103285+13$19.50

that limit the growth of a wetting layer to a large but finite value), and this phenomenon leads to modifications of equation (1) for large but finite L [12–19]. Parry and Evans [18] have suggested that in leading order the effect of the wetting layer can be expressed by replacing equation (1) with

$$\Delta\mu = [2\sigma_{lg}/(\rho_l - \rho_g)]/(L - \phi l) \qquad L \to \infty \tag{2}$$

where l is the thickness of the wetting film and for short-range wall forces the constant ϕ is $\phi = 2$ in $d = 3$ dimensions while it is $\phi = 3$ in $d = 2$ dimensions (where both the confining walls and the gas–liquid interfaces of the wetting layers are one-dimensional, of course). In view of a gas–liquid condensation in confined films in $d = 2$ we have, of course, ignored the fact that the system is quasi-one-dimensional and hence in the strict sense there is no longer any sharp phase transition [24–26]. The reason why the resulting rounding of the transition can be ignored is because the region $\delta\mu$ (or δT when one crosses the coexistence curve by varying the temperature T, respectively) over which the rounding occurs is extremely small [24–26], namely of the order of $L^{-3/2}\exp(-L\sigma_{lg}/k_BT)$. Physically this rounding is due to the fact that the one-dimensional strip has no true long-range order but rather breaks up into domains of extent $\xi_\parallel \propto L^{1/2}\exp(L\sigma_{lg}/k_BT)$ [24–26]. For large L this lateral linear dimension $\xi_\parallel$ in the direction parallel to the confining boundaries is so large that it is of practical relevance neither for experiment nor for simulations [17]. Note that the case $d = 2$ may be practically relevant for phase transitions in monolayers adsorbed at stepped surfaces, where terraces of width L bounded by parallel steps can be produced experimentally and act as substrates for adsorption [17, 27]. Of course, in this case one should consider the more general situation of two different boundary conditions at the terrace edges, since a step upward and a step downward are not equivalent.

While in equation (2) for the case $d = 3$ where $\phi = 2$ the effective thickness $L^* = L - 2l$ has the obvious geometrical interpretation that only the thickness L^* taken by the gas should be used in the 'Kelvin equation', equation (1), the situation in $d = 2$ is more subtle since $\phi = 3$ (this value results from strong interfacial fluctuations [18]) does not allow any obvious interpretation of the effective thickness $L^* = L - 3l$. Furthermore, one expects a singular (power-law type) variation of the thickness of the wetting layer at coexistence [17, 18] in the strip of thickness L, since the thickness of the wetting layer in a semi-infinite system diverges as $l \propto (\Delta\mu)^{-1/3}$ as $\Delta\mu \to 0$, and at the transition $\Delta\mu$ scales like $1/L$ for a strip (equation (1)). This yields

$$l \propto L^{1/3} \propto (\Delta\mu)^{-1/3} \qquad L \to \infty \tag{3}$$

while in $d = 3$ the corresponding variation is only logarithmic [17–19].

While in previous work [17] capillary condensation in the two-dimensional lattice gas with nearest-neighbour interactions has already been studied by Monte Carlo simulations, data were only taken relatively close to the bulk critical temperature T_{cb} ($T/T_{cb} \geqslant 0.95$, where the bulk correlation length ξ_b is already considerably larger than the lattice spacing) and for thin strips ($L \leqslant 36$ for $T/T_{cb} = 0.95$); these data are clearly not in the asymptotic regime of equations (2) and (3) and hence the test of equation (2) proposed by [18] turned out not to be meaningful. In the present work, we reconsider this problem, extending the simulation studies to lower temperatures and larger linear dimensions L, to clarify the applicability of equation (2).

In section 2, we briefly describe the model and techniques of simulation and analysis of the Monte Carlo 'data', while in section 3 we present our results. We conclude in section 4 with a discussion of the possible reasons for our failure to find any clear evidence for equation (2) from our model simulations.

2. Some background on the model and the techniques of simulation and analysis

Here we are not concerned with the study of a realistic model of some particular material but rather study the generic case of the nearest-neighbour Ising (lattice-gas) model [17, 19, 27]. Because of its simplicity, the model has distinctive advantages: (i) The discreteness of the lattice and the short range of the interactions allows rather fast simulation codes. (ii) What is more important, the location of the transition in the bulk ($\mu_{\rm coex}$) is known exactly, it corresponds to the case of bulk magnetic field $H = 0$ in the transcription to the corresponding Ising ferromagnet [19]. (iii) Also the location of the wetting transition in the presence of local boundary terms ('surface magnetic field' H_1 in the magnetic notation [17, 19, 27, 28] is known from exact calculations [29],

$$\exp(2J/k_{\rm B}T)[\cosh(2J/k_{\rm B}T) - \cosh(2H_1^{\rm w}/k_{\rm B}T] = \sinh[2J/k_{\rm B}T] \tag{4}$$

$J(>0)$ being the exchange interaction of the Ising ferromagnet, and $H_1^{\rm w}(T)$ describes the second-order wetting transition of a semi-infinite system (figure 1). For completeness and the sake of easier understanding, we quote the Hamiltonian first in 'magnetic notation',

$$\mathcal{H}_I = -J\sum_{\langle i,j\rangle} S_i S_j - H \sum_{\substack{i \\ \text{all spins}}} S_i - H_1 \sum_{i \text{ in layer } 1} S_i - H_1 \sum_{i \text{ in layer } L} S_i \tag{5}$$

where the Ising spins $S_i = \pm 1$, the sum $\langle i, j\rangle$ is taken once over all nearest-neighbour pairs in the lattice (note that in layers from $n = 2$ to $n = L - 1$ there are four nearest neighbours but in layers $n = 1$ and $n = L$ there are only three, due to the free boundaries at the edges of the system). Of course, Monte Carlo simulations cannot deal with $L \times \infty$ strips, so we actually simulate a $L \times M$ geometry but with $M \gg L$ and a periodic boundary condition in the 'long' direction of the system. Linear dimensions used are in the range $32 \leqslant L \leqslant 120$ and $M = 6L$ except for the case $H_1/J = 0.75$, $T/T_{\rm c} = 0.85$ where both $M = 6L$ and $M = 12L$ were used (within statistical errors no difference could be detected).

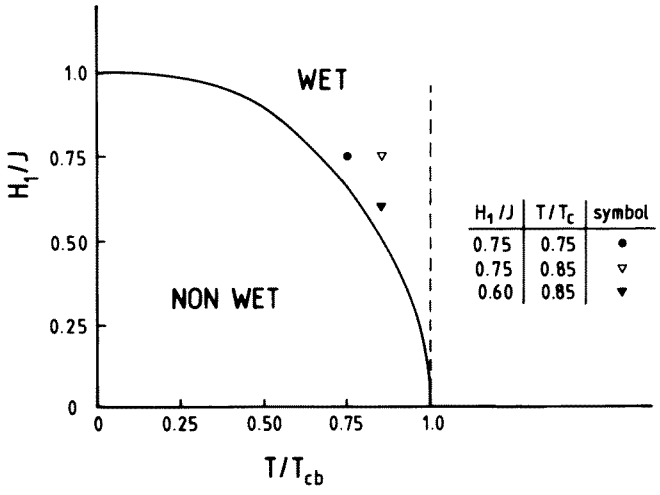

Figure 1. A surface phase diagram of a semi-infinite Ising (or lattice gas) model. In the plane of reduced temperature $T/T_{\rm cb}$ and reduced surface magnetic field H_1/J the wetting transition at $H_1^{\rm w}(T)$, shown as a full curve, equation (4), separates the nonwet states from the wet states of the surface. The symbols indicate the state points where simulations of capillary condensation have been performed in the present work: $T/T_{\rm cb} = 0.75$, $H_1/J = 0.75$ (full dot); $T/T_{\rm cb} = 0.85$, $H_1/J = 0.75$ (open triangle); $T/T_{\rm cb} = 0.85$, $H_1/J = 0.60$ (full triangle).

As is well known [17–19, 27], equation (5) is equivalent to the lattice gas problem, where lattice sites i can be occupied (concentration variable $c_i = 1$) or empty ($c_i = 0$), if one makes the identification $c_i = (1 - S_i)/2$, μ being the chemical potential,

$$\mathcal{H}_{\rm lg} = -\varphi \sum_{\langle i,j \rangle} c_i c_j - \varepsilon_1 \sum_{i \text{ in layer } 1} c_i - \varepsilon_1 \sum_{i \text{ in layer } L} c_i \tag{6}$$

$$\mathcal{H}_{\rm lg} = -\mu \sum_i c_i = \mathcal{H}_I + \mathcal{H}_0 \tag{7}$$

$\mathcal{H}_0$ being a constant that only shifts the origin of the energy scale, and the pairwise energy φ and boundary energy ε_1 are related to J and H_1 as follows,

$$\varphi = 4J \qquad \varepsilon_1 = 2J - 2H_1 \tag{8}$$

while μ is related to the magnetic field ($\mu = -2H - 8J$, i.e. phase coexistence in the bulk occurs for $\mu_{\rm coex} = -8J$). Equation (8) shows that in the lattice gas a boundary potential (ε_1 arises also when $H_1 = 0$ in the corresponding Ising magnet ('missing neighbour effect'). Conversely, even if the boundary potential ε_1 is zero, we have to work with $H_1 \neq 0$ in the Ising magnet.

Monte Carlo simulations have been carried out with a standard single spin flip algorithm, taking 10^4 Monte Carlo steps (MCS) per site, the first 2.5×10^3 MCS being discarded for equilibration. These times are relatively short and thus our results still show noticeable statistical errors but for the system sizes involved (for $L = 120$ our lattice contains 86 400 spins) we have to take data at many values of the thermodynamic integration, and thus altogether the calculation already involves a total investment of computer time of the order of 10^3 workstation hours.

The quantities recorded are profiles of the local density ρ_n across the film, as well as the average density $\bar{\rho} = (\sum_{n=1}^{L} \rho_n)/L$ and the average energy $\bar{E}$ per lattice site in the Ising magnet representation, $\bar{E} = \langle \mathcal{H}_I \rangle / (LM)$. (Here the overbar stands for the averaging over all the layers n.) As an example, figures 2 and 3 show data for ρ_n which qualitatively resemble their three-dimensional counterparts (cf [19]). The layer densities ρ_n are the thermal averages of the concentration variables for lattice sites in the respective layer, $\rho_n = \langle c_i \rangle$ for i in layer n.

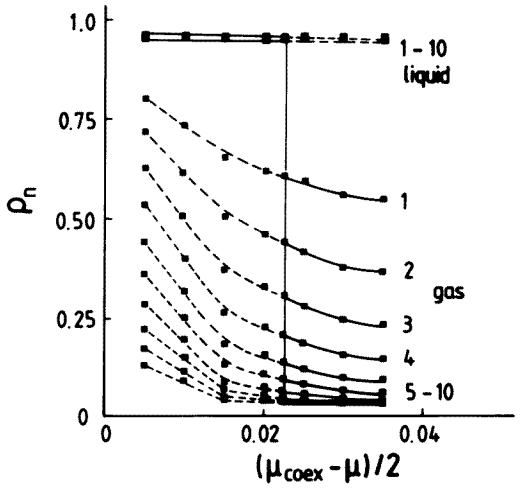

Figure 2. Layer densities ρ_n, for $n = 1, \ldots, 10$, plotted versus chemical potential difference $(\mu_{\rm coex} - \mu)/2J (= H/J)$, for the case $H_1/J = 0.60$, $T/T_{\rm cb} = 0.85$, $L = 72$ and $M = 432$. Note that pronounced hysteresis between the liquid phase and the gas phase is observed. The actual transition point $\mu_{\rm c}(L)$ is determined from thermodynamic integration methods, and shown here by a straight vertical line.

As expected, a pronounced hysteresis occurs at the first-order gas–liquid condensation transition, see figure 2, making a straightforward estimation of the chemical potential $\mu_{\rm c}(L)$

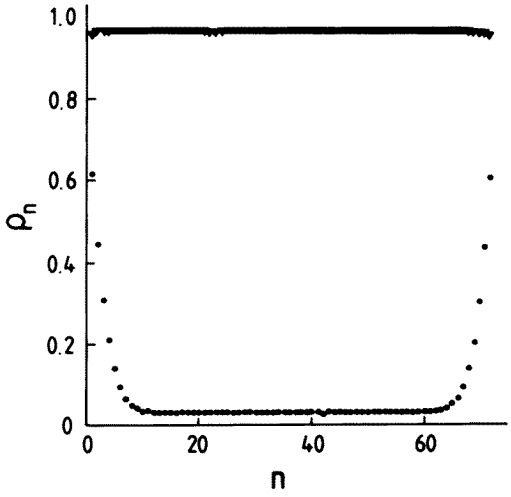

Figure 3. Layer densities ρ_n plotted versus the layer number n for the case $H_1/J = 0.60$, $T/T_{cb} = 0.85$, $L = 72$ and $M = 432$, at phase coexistence $\{[(\mu_{coex} - \mu_c(L)]/2J = 0.0224\}$. The liquid branch is shown by open symbols, the gas branch by full symbols. Note the density enhancement near both walls.

where the transition is difficult. We thus have followed [19], by applying thermodynamic integration methods. Note that thermodynamic integration methods are necessary, since Monte Carlo simulation methods straightforwardly yield derivatives of thermodynamic potentials only (such as the average density $\bar{\rho}$ and the average energy $\bar{E}$ of the thin film), but neither the entropy nor any of the relevant thermodynamic potentials (average free energy $\bar{F}$ or grand potential $\bar{\Omega}$ of the thin film) is a direct output of a Monte Carlo simulation. Thermodynamic integration now means that one exploits a relation such as $\bar{E} = (\partial \bar{F}/\partial\beta)_\mu$ to obtain the free energy $\bar{F}$ of a state at temperature $T = 1/\beta k_B$ and chemical potential μ as

$$\beta\bar{F} = \beta\bar{F}_0 + \int_{\beta_0}^{\beta} \bar{E}(\beta')\mathrm{d}. \tag{9}$$

The starting temperature $T_0 = 1/\beta_0 k_B$ has to be chosen close to zero temperature, such that the entropy is negligible, $\bar{F}_0 \approx \bar{E}_0$. Now, in principle it would be possible to choose one state at a chemical potential μ_1 in the liquid phase, the other state at another chemical potential μ_2 in the gas phase, and obtain the free energies $\bar{F}_1(T, \mu_1)$ and $\bar{F}_2(T, \mu_2)$ of the two states, as well as their grand potentials $\bar{\Omega}_1(T, \mu_1) = \bar{F}_1 - \bar{\rho}_l\mu_1$, $\bar{\Omega}_2(T, \mu_2) = \bar{F}_2 - \bar{\rho}_g\mu_2$. Next we could use these states on an isotherm at fixed temperature T as reference states to calculate grand potential differences from

$$\begin{aligned} \bar{\Omega}_1(T, \mu) &= \bar{\Omega}_1(T, \mu_1) - \int_{\mu_1}^{\mu} \bar{\rho}_l(\mu')\,\mathrm{d}\mu' \\ \bar{\Omega}_2(T, \mu) &= \bar{\Omega}_2(T, \mu_2) - \int_{\mu_2}^{\mu} \bar{\rho}_g(\mu')\,\mathrm{d}\mu'. \end{aligned} \tag{10}$$

Then the phase transition is located by finding the chemical potential where the grand potentials are equal, $\bar{\Omega}_1(T, \mu) = \bar{\Omega}_2(T, \mu)$.

In practice, for large D the thermodynamic potentials in the two states close to phase coexistence differ very little, however, and hence the method would be very sensitive to errors resulting from inaccuracies involved in the numerical integration in equation (9), where one has to integrate over a rather wide range ($T_0 = 0.25T_c$ was chosen in practice). Thus, we choose a slight variation of this technique [19], where one considers the free

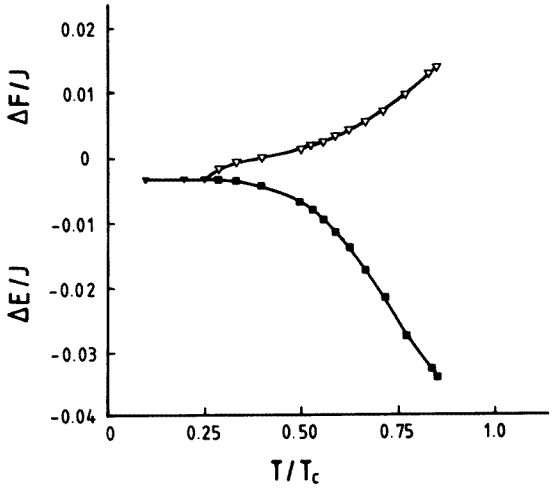

Figure 4. Energy difference per site $\Delta E/J$ between the liquid and the gas branch (full symbols) and corresponding free energy difference (open symbols) plotted versus the reduced temperature, for the case $H_1/J = 0.60$, $T/T_c = 0.85$, $L = 72$, $M = 432$, and bulk field $H/J = 0.005$ (liquid branch) and $H/J = 0.025$ (gas branch), respectively. The final result for the free energy difference $\Delta F/J$ at $T/T_c = 0.85$ is $\Delta F/J \approx 1.38 \times 10^{-2}$.

energy difference $\Delta F = \bar{F}_2 - \bar{F}_1$ between the two states at μ_1, μ_2, and carries out a single integration over inverse temperatures only,

$$\beta(\Delta F) = \beta_0(\Delta F_0) + \int_{\beta_0}^{\beta} \Delta E(\beta')\,\mathrm{d}\beta \qquad \text{with } \Delta E = \bar{E}_2 - \bar{E}_1.$$

As an example, figure 4 shows both ΔE and ΔF as functions of temperature for a typical case. Although the total energy per lattice site (in units of J) clearly is always of the order of unity, the energy difference $\Delta E(\beta)$ for our lattice site is of the order of 10^{-2}, and correspondingly small free energy differences ΔF result. By the present techniques, however, it is possible to locate the transition point with reasonable accuracy (figure 5). In applying equation (10), this then means we do not work directly with the grand potentials $\bar{\Omega}_1(T, \mu), \bar{\Omega}_2(T, \mu)$ themselves, but with grand potential differences $\Delta\bar{\Omega}_1 \equiv \bar{\Omega}_1(T, \mu) - \bar{\Omega}_{\mathrm{RP}}$, $\Delta\Omega_2 \equiv (T, \mu) - \bar{\Omega}_{\mathrm{RP}}$, where the grand potential $\bar{\Omega}_{\mathrm{RP}}$ in a reference point RP (which we choose at T, μ_1 at the liquid branch) is subtracted (therefore the liquid branch (LB) in figure 5 at the reference point starts at zero by construction, and the small differences—$\Delta\Omega_1/J$, $\Delta\Omega_2/J$ are both of the order of 10^{-2} as well—are obtained with meaningful accuracy).

Since equation (2) proposes a relation between the shift $\Delta\mu$ of the transition and a reduced thickness $\tilde{L} = L - \phi l$, where it was suggested [18] that $\phi = 3$ in $d = 2$ dimensions and l is the thickness of the wetting layer at the transition, it also is of interest to estimate the latter. This can be done in terms of the surface excess density ρ_{s} as follows [30]

$$l = \rho_{\mathrm{s}}/(\rho_{\mathrm{l}}^{\mathrm{coex}} - \rho_{\mathrm{g}}^{\mathrm{coex}}) \tag{11}$$

where ρ_{s} can be expressed in terms of the layer densities ρ_n at the gas branch as

$$\rho_{\mathrm{s}} = \tfrac{1}{2}\sum_{n=1}^{\mathrm{L}}(\rho_n - \rho_{\mathrm{b}}) \qquad \rho_{\mathrm{b}} = \sum_{n=L/2-4}^{L/2+5} \rho_n/10. \tag{12}$$

Note that by definition the surface excess density ρ_{s} can be related to the average density $\bar{\rho}$ by writing $\bar{\rho} = \rho_{\mathrm{b}} + (2/L)\rho_{\mathrm{s}}$, as is well known [30]. In order to gain statistics, the bulk density ρ_{b} is defined in terms of an average over the 10 innermost layers. For $L \to \infty$ we have at the transition $\rho_{\mathrm{b}} = \rho_{\mathrm{g}}^{\mathrm{coex}}$, while for finite L $\mu_{\mathrm{c}}(L) \neq \mu_{\mathrm{coex}}$, and then ρ_{b} will be systematically smaller than the gas density $\rho_{\mathrm{g}}^{\mathrm{coex}}$ for bulk phase coexistence (for boundaries

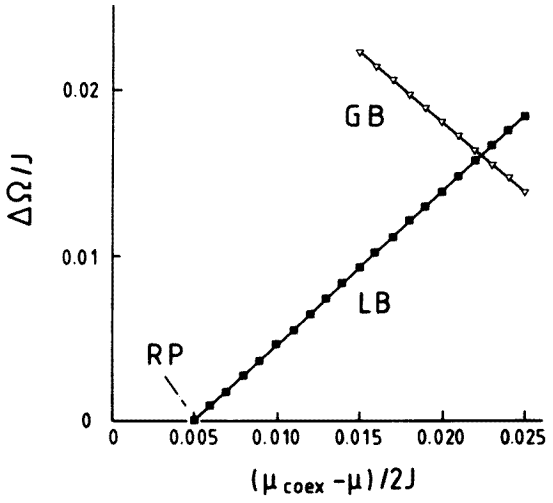

Figure 5. Grand potential difference $\Delta\Omega/J$ per lattice site, with respect to the reference point (RP) at $(\mu_{\rm coex} - \mu)/2J = 0.005$ at the liquid branch (LB), plotted as a function of the reduced chemical potential difference. Data for the liquid branch are shown by full symbols and for the gas branch (GB) by open symbols. The crossing point ($\Delta\Omega_1 = \Delta\Omega_2$) yields the transition point, $\mu = \mu_{\rm c}(L)$.

Table 1. Chemical potential shift $\Delta\mu$ and gas excess density $\rho_{\rm sc}$ at the condensation transition tabulated for various film thicknesses.

	$H_1/J = 0.75, T/T_{\rm c} = 0.85$		$H_1/J = 0.75, T/T_{\rm c} = 0.75$		$H_1/J = 0.60, T/T_{\rm c} = 0.85$	
L	$\Delta\mu$	$\rho_{\rm sc}$	$\Delta\mu$	$\rho_{\rm sc}$	$\Delta\mu$	$\rho_{\rm sc}$
32	0.0528	1.499	0.046 6	1.019	0.0760	0.721
40	0.0371	1.917	0.031 4	1.337	0.0485	1.032
48	0.0258	2.463	0.020 95	1.690	0.0310	1.378
60	0.0191	2.962	0.017 95	1.948	0.0274	1.526
72	0.0179	3.105	0.014 6	2.154	0.0224	1.744
96	0.0123	3.886	0.009 15	2.839	0.0150	2.280
120	0.0120	3.953	0.008 0	3.177	—	—

that prefer the fluid phase). An inspection of figure 3 readily shows that for our choice of parameters the liquid density at coexistence $\rho_{\rm l}^{\rm coex}$ is close to its saturation value unity, and $\rho_{\rm g}^{\rm coex}$ is nearly zero. Thus l exceeds $\rho_{\rm s}$ by a few per cent only.

3. Results of the shift of the condensation transition and of the corresponding precursor wetting layer

Table 1 lists the results that we have obtained for $\Delta\mu \equiv (\mu_{\rm coex} - \mu_{\rm c}(L)/(2J))$ and the excess density $\rho_{\rm sc}$ of the gas branch at the first-order transition. Figure 6 plots $\Delta\mu$ as function of $1/L$, to show that roughly one does have consistency with the simple Kelvin equation, for large enough L, while when one includes smaller L a pronounced smooth curvature is seen on this plot. Figure 7 shows that this curvature can be interpreted in terms of an offset L_0 in the Kelvin equation, $\Delta\mu(L) = C/(L - L_0)$. Should one interpret this offset L_0 as a consequence of the proposed modification of the Kelvin equation, equation (2)? In order to check this possibility, figure 8 plots $(\Delta\mu L)^{-1}$ versus $L^{-2/3}$, since equations (2) and (3) imply that in this representation there should be a linear variation,

$$(\Delta\mu L)^{-1} \propto (1 - \phi l/L) = (1 - \text{constant } L^{-2/3}) \qquad L \to \infty. \tag{13}$$

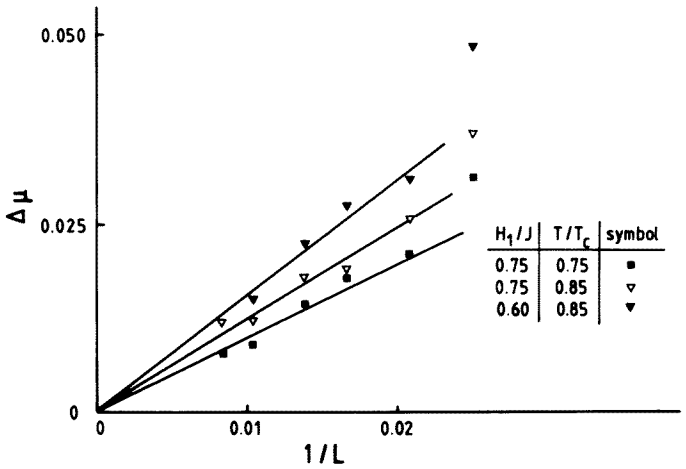

Figure 6. Shift of the reduced chemical potential at the transition, defined as $\Delta\mu \equiv (\mu_{coex} - \mu_c(L)/2$, plotted as a function of $1/L$, for $H_1/J = 0.75$, $T/T_c = 0.76$ (squares), $H_1/J = 0.75$, $T/T_c = 0.85$ (open triangles), and $H_1/J = 0.6$, $T/T_c = 0.85$ (full triangles). The straight lines indicate fits of the data for $L \geqslant 48$ to the Kelvin equation, $\Delta\mu \propto 1/L$. Note that data for $L = 32$ are off the scales of this plot and have not been included here.

Unfortunately, figure 8 shows considerable scatter which masks possibly also some curvature, and thus it cannot really be claimed that the data provide clear evidence for equation (2). However, the data should not be taken as evidence against the asymptotic validity of equation (2) either, simply because it is possible that we are in a parameter range where $\Delta\mu$ is still too large, and l is too small for equation (2) to be valid. Such a caveat must be made considering the fact that ρ_{sc} is in the range from about 1 to 4 (table 1), and thus also l is in the range from 1 to 4 lattice spacings. This is clearly too small to verify at least the asymptotic behaviour for the thickness of the wetting layer, equation (3), as figure 9(a) shows: while the data for ρ_{sc} versus $\Delta\mu$ seem to be compatible with a simple power law, the exponent is twice as large as that predicted! And the data for ρ_{sc} versus L also give too large 'effective' exponents but there is some evidence for a curvature in the direction of smaller effective exponents, and it is possible that for $H_1/J = 0.75$, $T/T_c = 0.85$ the correct asymptotic behaviour has been reached for the two largest sizes. We do not understand, however, why the plot of ρ_{sc} versus $\Delta\mu$ does not exhibit the least sign of a corresponding crossover. We recall that related problems for critical rather than complete wetting (the exponents for critical wetting in $d = 2$ are seen only extremely close to the transition) are reported in [28]. And surprisingly, ρ_{sc} is rather well consistent with a simple logarithmic variation, $\rho_{sc} \approx bln(L/L_0)$, where b and L_0 are constants, figure 9(b) (note that L_0 in figure 9(b) is the same constant as in figure 7(b)).

The physical reason why precursor wetting layers having a thickness of a few lattice spacings are not suitable to verify equation (3) is that the width of local fluctuations of the interface is also a few lattice spacings, and hence a fully connected precursor wetting layer at the boundary does not yet exist under these conditions, rather one finds a sequence of irregular droplets attached to the boundary. This fact is readily seen from snapshot pictures of the lattice gas (figure 10). So the standard picture involved in the theoretical description [18], where one models the essential degrees of freedom in terms of two contours $l(x)$ describing the local distance of the interface from the boundaries, x being a coordinate along the boundaries, clearly does not apply, since the capillary wave Hamiltonian, that

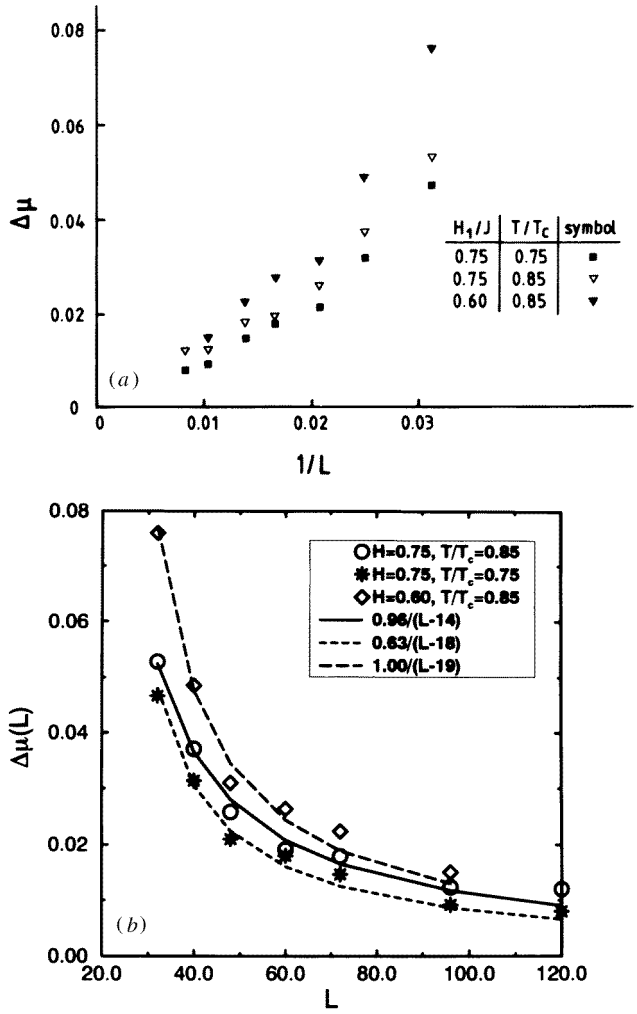

Figure 7. Plot of $\Delta\mu(L)$ versus L, showing least square fits to a law $\Delta,\mu(L) = C/(L - L_0)$, with constants C, L_0 quoted in the figure.

is then invoked, implies that $l(x)$ has only weak long wavelength fluctuations. While we do not exclude that such a picture may become valid for much larger film thicknesses L, where $\rho_{sc} \gg 1$, on a suitably coarse-grained scale, figure 10 gives clear evidence that this picture does not apply for our range of parameters. In this respect, the present problem differs from many other properties of the Ising model, for example bulk critical behaviour where asymptotic laws can already be deduced when the correlation length is only a few lattice spacings. Nevertheless, recognizing the fact that l does not yet scale according to equation (3), it is still conceivable that equation (2) is a useful improvement over the simple Kelvin equation, if one takes the actual l (or ρ_{sc}, respectively) observed in the simulation in that equation. Thus, plotting $(\Delta\mu L)^{-1}$ versus ρ_{sc}/L we expect simple straight lines, cf equation (13). However, plotting our data in this way (figure 11) we only observe a huge scatter, much worse than in the corresponding plot $(\Delta\mu L)^{-1}$ versus $L^{-2/3}$ (figure 8). It does seem unlikely to us that this large scatter reflects simply our statistical and systematic

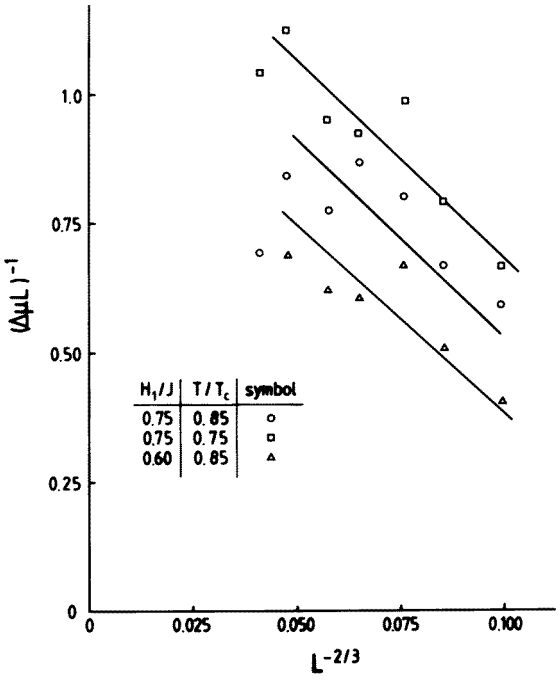

Figure 8. Plot of $(\Delta\mu L)^{-1}$ versus $L^{-2/3}$. The meaning of the symbols is the same as in figure 6.

errors, since the data used for this plot (figures 8 and 9) were distinctly smoother. We rather feel that equation (2) in our parameter range (where l and ρ_{sc} are still rather small) simply is not yet applicable.

4. Discussion

In this paper we have studied the shift of the first-order gas–liquid phase transition induced by short-range boundary effects on a nearest-neighbour two-dimensional lattice gas model. Strips of width L, with $32 \leqslant L \leqslant 120$, have been considered at two temperatures, $T = 0.75T_c$ and $T = 0.85T_c$, choosing surface fields such that one is clearly on the wet side of the critical wetting transition.

While our data are roughly compatible with the Kelvin equation in its simplest form, $\Delta\mu \propto L^{-1}$, or with a constant offset, $\Delta\mu \propto (L - L_0)^{-1}$, we see no clear evidence for the proposed relation, $L = 3l$ (equation (2)). Of course, this conclusion is somewhat tentative, in view of considerable statistical errors still present in some of the data (figures 8 and 9), and possible systematic errors since our aspect ratio M/L is still finite ($M/L = 6$) rather than infinite (in one case data for $M/L = 12$ were generated as well, and no clear sign of a systematic difference could be detected). Another systematic effect could be that much longer runs need to be carried out to fully develop the long-range capillary wave fluctuation spectrum, but again we have no positive indication that finite observation time effects severely hamper our results. On the other hand, there seems rather clear evidence from the data (figures 9 and 10) that under the present conditions there are not yet clearly developed precursor wetting layers bound to the boundary, but rather the boundary gets 'decorated' more and more with irregular droplets as L increases. Of course, this would be a description of a *nonwet* boundary, for which the simple Kelvin equation (equation (1)) is believed to hold anyway. In this sense, our findings for the shift of the transition and

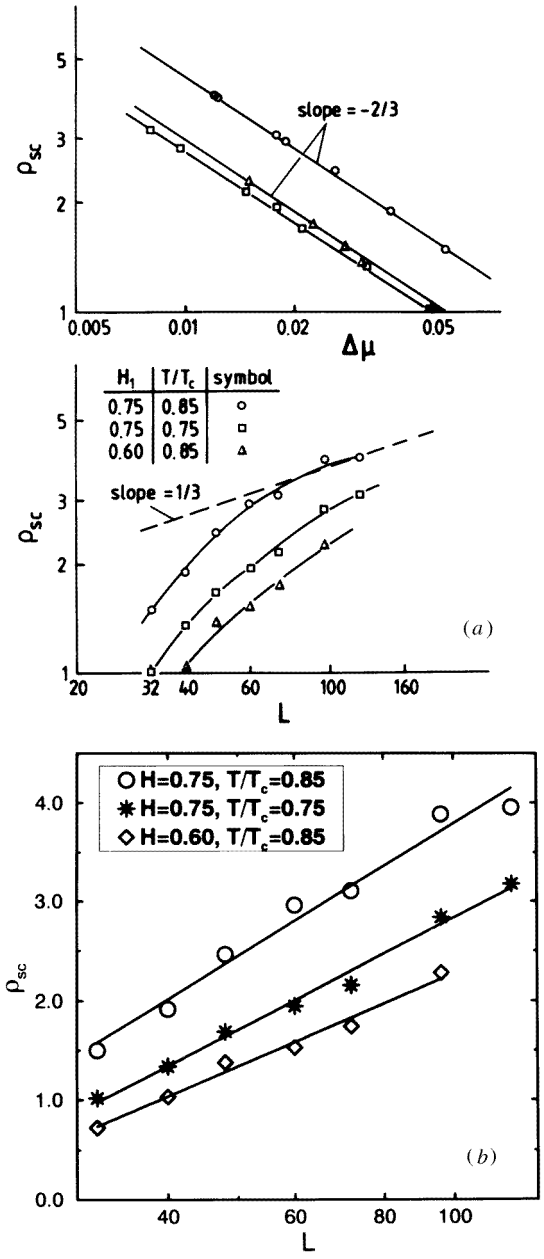

Figure 9. (*a*) Log–log plot of the surface excess densities at the condensation transition of ρ_{sc} versus $\Delta\mu$ (upper part) and of ρ_{sc} versus L (lower part). Note that the theoretical behaviour (equations (3) and (11)) is $\rho_{sc} \propto (\Delta\mu)^{-1/3}$, $\rho_{sc} \propto L^{1/3}$. In the lower part the broken straight line indicates such an expected behaviour. (*b*) Semi-log plot of ρ_{sc} versus L.

its size dependence are well compatible with the microscopic analysis of our system. The interpretation of our findings hence is that for the studied range of sizes the 'bulk field' H present at the transition is still so strong that it eliminates the wet character of the boundary (present at $H = 0$) more or less completely, making it appear to be essentially nonwet, although for $H \to 0$ it is wet. As a consequence, extremely large thickness L (beyond the reach of our simulations) would be needed to test equation (2). If this conclusion is not only true for our nearest-neighbour lattice gas but generic for a broad class of physical systems, the implication would be that the general theoretical description of wetting phenomena does

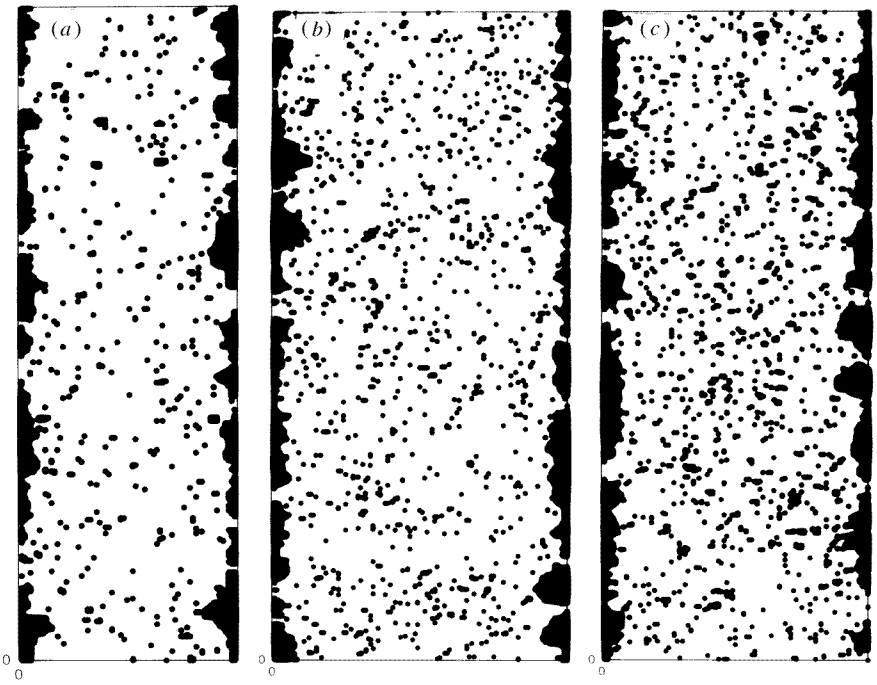

Figure 10. Snapshot pictures of the lattice gas for $\mu = \mu_c(L)$ and $T/T_c = 0.75$, $H_1/J = 0.75$, for (*a*) $L = 72$, (*b*) $L = 120$ and (*c*) $L = 96$, $T/T_c = 0.85$, $H_1/J = 0.60$.

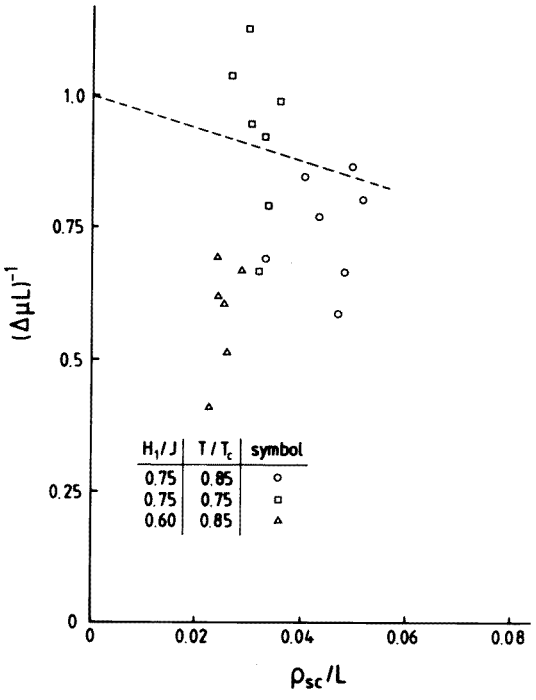

Figure 11. Plot of $(\Delta\mu L)^{-1}$ versus ρ_{sc}/L. Note that the theoretical expectation (equations (2) and (3)) is that the data should fall on three straight lines which all have a positive intercept and a gradient close to $-\phi = -3$ since ρ_{sc} is only slightly smaller than l. Such a line is included for illustration only.

have a limited validity for describing wetting effects on capillary condensation transition only.

Clearly, it would be of interest to look into this problem by using other suitable techniques, to estimate for which lengths L (or l, respectively) one enters the regime where equation (2) holds, and to develop a better theoretical understanding for the regime where l is still small. We feel that this might also be useful for interpreting experiments.

Acknowledgments

This work was supported in part by the Alexander von Humboldt-Stiftung, the Deutsche Forschungsgemeinschaft (DFG), grant no SFB262/D1, and by the Volkswagen Stiftung (grant no I/69078).

References

[1] Fisher M E 1971 Critical phenomena *Proc. Enrico Fermi International School of Physics* vol 51, ed M S Green (New York: Academic)
[2] Barber M N 1983 *Phase Transitions and Critical Phenomena* vol 8, ed C Domb and J L Lebowitz (New York: Academic) p 146
[3] Binder K 1987 *Ferroelectrics* **73** 43
[4] Cardy J L (ed) 1988 *Finite Size Scaling* (Amsterdam: North-Holland)
[5] Privman V (ed) 1990 *Finite-Size Scaling and Numerial Simulations of Statistical Systems* (Singapore: World Scientific)
[6] Binder K 1992 *Computational Methods in Field Theory* ed H Gausterer and C B Lang (Berlin: Springer) p 59
[7] Binder K 1992 *Ann. Rev. Phys. Chem.* **43** 33
[8] Zsigmondy R 1911 *Z. Anorg. (Allg.) Chem.* **71** 356
[9] Fisher M E and Nakanishi H 1981 *J. Chem. Phys.* **75** 1981
[10] Nakanishi H and Fisher M E 1983 *J. Chem. Phys.* **78** 3279
[11] Evans R 1990 *J. Phys.: Condens. Matter* **2** 8989
[12] Derjaguin B V 1940 *Acta. Phys. Chem.* **12** 181
[13] Evans R and Marini Bettolo Marconi U 1985 *Chem. Phys. Lett.* **114** 415
[14] Evans R, Marini Bettolo Marconi U and Tarazona P 1986 *J. Chem. Soc. Faraday. Trans.* II **82** 1763
Evans R, Marini Bettolo Marconi U and Tarazona P 1987 *J. Chem. Phys.* **86** 7138
[15] Lipowsky R and Gompper G 1984 *Phys. Rev.* B **29** 5213
Sornette D 1985 *Phys. Rev.* B **31** 4672
[16] Nicolaides D and Evans R 1989 *Phys. Rev.* B **39** 9336
[17] Albano E V, Binder K, Heermann D W and Paul W 1989 *J. Chem. Phys.* **91** 3700
[18] Parry A O and Evans R 1992 *J. Phys. A: Math. Gen.* **25** 275
[19] Binder K and Landau D P 1992 *J. Chem. Phys.* **96** 1444
[20] Sullivan D E and Telo da Gama M M 1986 *Fluid Interfacial Phenomena* ed C A Croxton (New York: Wiley) p 45
[21] Dietrich S 1988 *Phase Transitions and Critical Phenomena* vol 12, ed C Domb and J L Lebowitz (New York: Academic) p 1
[22] Schick M Liquids at interfaces *Les Houches Session XLVIII* ed J Charvolin, J F Joanny and J Zinn-Justin (Amsterdam: North-Holland) p 415
[23] Thomson W 1871 *Phil. Mag.* **42** 44
[24] Fisher M E 1969 *J. Phys. Soc. Japan. Suppl.* **26** 87
[25] Privman V and Fisher M E 1983 *J. Stat. Phys.* **33** 385
[26] Cabrera G C, Jullien R, Brezin E and Zinn-Justin J 1986 *J. Physique* **47** 1305
[27] Albano E V, Binder K, Heermann D W and Paul W 1989 *Surf. Sci.* **223** 151
[28] Albano E V, Binder K, Heermann D W and Paul W 1990 *J. Stat. Phys.* **61** 161
[29] Abraham D B 1980 *Phys. Rev. Lett.* **44** 1165
[30] Binder K 1983 *Phase Transitions and Critical Phenomena* vol 8, ed C Domb and J L Lebowitz (New York Academic) p 1